Preprint typeset in JHEP style - HYPER VERSION
hep-ph/0507041, TTP05–07, SFB/CPP-05-17 — July 2005

Pseudo-scalar Higgs production at next-to-leading order SUSY-QCD

Robert V. Harlander and Franziska Hofmann

Institut für Theoretische Teilchenphysik, Universität Karlsruhe
D-76128 Karlsruhe, Germany
E-mail: robert.harlander@cern.ch, fhofmann@particle.uni-karlsruhe.de

Abstract: The production rate of the CP-odd Higgs boson in the Minimal Supersymmetric Standard Model is evaluated through next-to-leading order in the strong coupling constant. The divergent integrals are regulated using Dimensional Reduction, with a straightforward implementation of γ_5. The well-known Standard Model result is recovered in this scheme through a cancellation between the quark and squark contributions as the masses of the supersymmetric particles tend to infinity.

Keywords: Higgs production, hadron collider, supersymmetry, next-to-leading order calculations.

Contents

1. Introduction **1**

2. Notation and Leading Order Result **3**

2.1 Lagrangian 3

2.2 Hadronic cross section 3

2.3 Standard Model limit and leading order result 4

3. Higher orders **5**

3.1 Standard Model result – Effective Lagrangian 5

3.2 SUSY contributions 6

4. Results **7**

5. Discussion **9**

5.1 Coefficient function $\tilde{C}_1$ 9

5.2 Cross section 10

6. Conclusions **13**

1. Introduction

The MSSM predicts a fundamental CP-odd scalar particle A, commonly referred to as the pseudo-scalar Higgs boson. One of the most important properties that distinguishes it from its CP-even analogues h and H is the absence of tree-level couplings to the electro-weak gauge bosons W and Z. Decay and production processes through these particles, which have been shown to be extremely helpful for CP-even Higgs searches and studies, are thus very much suppressed. This leaves associated $t\bar{t}A$ and $b\bar{b}A$ production as well as the loop-induced gluon fusion process as the most important production modes of a pseudo-scalar Higgs boson at the LHC (for a recent review, see Ref. [1]). In this paper, we present the evaluation of the inclusive gluon fusion cross section through NLO in the strong coupling constant.

Despite the fact that the tree-level $gg\phi$ coupling vanishes ($\phi \in \{h, H, A\}$), gluon fusion in general has a comparatively large cross section due to the high gluon luminosity at the LHC, and the large top-Yukawa coupling. In the limit where squarks and gluinos are decoupled, QCD corrections have been evaluated through NNLO [2, 3, 4, 5, 6]; they have been shown to be numerically significant but perturbatively well-behaved.

A precise determination of the gluon fusion cross section at the LHC could yield sensitivity to as yet undiscovered particles that may mediate the $gg\phi$ coupling apart from the top and bottom quarks. Within the MSSM, for example, top squarks can play a significant role if they are lighter than around 400 GeV (recall that the Yukawa coupling for squarks is typically proportional to m_q^2 rather than $m_{\tilde{q}}^2$). In the case of CP-even Higgs bosons, such effects occur already at LO (i.e., 1-loop). The NLO result was obtained in Ref. [7] within an effective theory for top, stop, and gluino masses much larger than the Higgs mass.

For the CP-odd Higgs boson, however, squarks do not affect the ggA vertex at 1-loop level due to the structure of the $A\tilde{q}\tilde{q}$ coupling, as will be shown below. The two-loop effects are thus expected to have a larger influence than for the CP-even Higgs production. What adds to this is that, in the limit of large m_q, the quark mediated contribution to the ggA vertex does not receive any QCD corrections due to the Adler-Bardeen theorem. As we will show, the only 2-loop QCD effects to this coupling are due to mixed gluino-quark-squark diagrams in this limit, leading to a potentially increased sensitivity to the gluino mass. Of course, the heavy quark limit is not applicable for the bottom mediated gluon-Higgs coupling which does receive QCD corrections [8, 9].

The calculation involves a technical issue that deserves special mention, namely the implementation of γ_5 within DRED. Its mathematically consistent and practically feasible formulation has been a subject of interest for many years now [10] (for recent developments concerning DRED, see Ref. [11, 12]). Here we adopt an approach close to the prescription of Refs. [13, 14]. An important consistency check is obtained from the SM limit: even for an infinitely heavy SUSY spectrum, the SUSY diagrams give a non-vanishing contribution which exactly cancels the 2-loop contributions arising from the SM diagrams in this scheme. The well-known result of vanishing higher order corrections to the quark-mediated ggA coupling, as required by the Adler-Bardeen theorem, is thus recovered in a non-trivial way. Combining this observation with the considerations of Ref. [12], it seems likely that in a supersymmetric theory the formal difficulties of DRED do not pose serious technical problems in practical calculations [10].

The outline of this paper is as follows: In Sect. 2 we introduce our notation and quote the LO result for the partonic process $gg \to A$. In Sect. 3, the effective Lagrangian underlying our calculation is introduced and the treatment of γ_5 is discussed. Sect. 4 outlines the method of the calculation and discusses the general structure of the result. It also provides the analytic formulae in some limiting cases. The numerical influence of the NLO terms is discussed in Sect. 5. In Sect. 6 our findings are summarized and an outlook on possible extensions of this work is given.

2. Notation and Leading Order Result

2.1 Lagrangian

We write the underlying Lagrangian in the following form:

$$\mathcal{L} = \mathcal{L}_{\rm QCD} + \mathcal{L}_{qA} + \mathcal{L}_{\rm SQCD} + \mathcal{L}_{\tilde{q}A}\,, \tag{2.1}$$

where

$$\mathcal{L}_{qA} = \sum_q \frac{m_q}{v}\, g_q^A\, \bar{q}\gamma_5 q A\,, \qquad \mathcal{L}_{\tilde{q}A} = \sum_q \sum_{i=1}^{2} \frac{m_q^2}{v}\, \tilde{g}_{q,ij}^A\, \tilde{q}_i\tilde{q}_j\, A\,. \tag{2.2}$$

The sums $\sum_q$ run over all quark flavors. m_q is the mass of quark q and $v \approx 246\,\text{GeV}$ the Higgs vacuum expectation value; the coupling constants g_q^A and $\tilde{g}_{q,ij}^A$ will be defined below. $\mathcal{L}_{\rm QCD}$ denotes the full QCD Lagrangian with six quark flavors, while $\mathcal{L}_{\rm QCD} + \mathcal{L}_{\rm SQCD}$ is the supersymmetric extension of $\mathcal{L}_{\rm QCD}$ within the MSSM, i.e., $\mathcal{L}_{\rm SQCD}$ incorporates kinetic, mass, mixing, and interaction terms of all the squarks and gluinos. Since we will be concerned with higher orders in the strong coupling α_s only, A does not appear as a dynamical field and does not require a kinetic term.

$\tilde{q}_1, \tilde{q}_2$ denote the squark mass eigenstates, related to the chiral eigenstates $\tilde{q}_L, \tilde{q}_R$ (the superpartners of the left- and the right-handed quark q) through

$$\begin{pmatrix} \tilde{q}_1 \\ \tilde{q}_2 \end{pmatrix} = \begin{pmatrix} \cos\theta_q & \sin\theta_q \\ -\sin\theta_q & \cos\theta_q \end{pmatrix} \begin{pmatrix} \tilde{q}_L \\ \tilde{q}_R \end{pmatrix}. \tag{2.3}$$

The coupling constants relevant for the following discussion are[1]

$$\begin{aligned} &g_b^A = \tan\beta\,, \qquad g_t^A = \cot\beta\,, \qquad \tilde{g}_{t,11}^A = \tilde{g}_{t,22}^A = 0\,, \\ &\tilde{g}_{t,12}^A = -\tilde{g}_{t,21} = \frac{m_{\tilde{t}_1}^2 - m_{\tilde{t}_2}^2}{2m_t^2}\,\sin\theta_t\,\cot\beta + \frac{\mu_{\rm SUSY}}{m_t}\,(\cot^2\beta + 1)\,. \end{aligned} \tag{2.4}$$

The effect of quarks other than bottom and top can be neglected due to their small Yukawa couplings; squark effects, on the other hand, are typically suppressed by at least one power of $m_q/m_{\tilde{q}}$, so that only top squarks will be considered in this paper.

2.2 Hadronic cross section

The cross section for the hadronic process $pp \to A + X$ at a center-of-mass energy s is determined by the formula[2]

$$\sigma(z) = \sum_{i,j\in\{q,\bar{q},g\}} \int_z^1 {\rm d}x_1 \int_{z/x_1}^1 {\rm d}x_2\, \varphi_i(x_1)\varphi_j(x_2)\,\hat{\sigma}_{ij}\left(\frac{z}{x_1 x_2}\right)\,, \qquad z := \frac{M_A^2}{s}\,, \tag{2.5}$$

[1]For a more complete collection of Feynman rules, see Ref. [15], for example.

[2]The modifications for $p\bar{p}$ collisions are obvious and shall not be pointed out explicitely in this paper.

where $\varphi_i(x)$ is the density of parton i inside the proton. $\hat{\sigma}_{ij}$ is the cross section for the process $ij \to A + X$, where, as indicated in Eq. (2.5), i and j are parton labels. For our numerical analysis, we will use the MRST parton density sets throughout this paper [16, 17].

Sample diagrams for i=j=g and i=g, j=q that contribute to the inclusive Higgs production rate at LO and NLO are shown in Fig. 1.

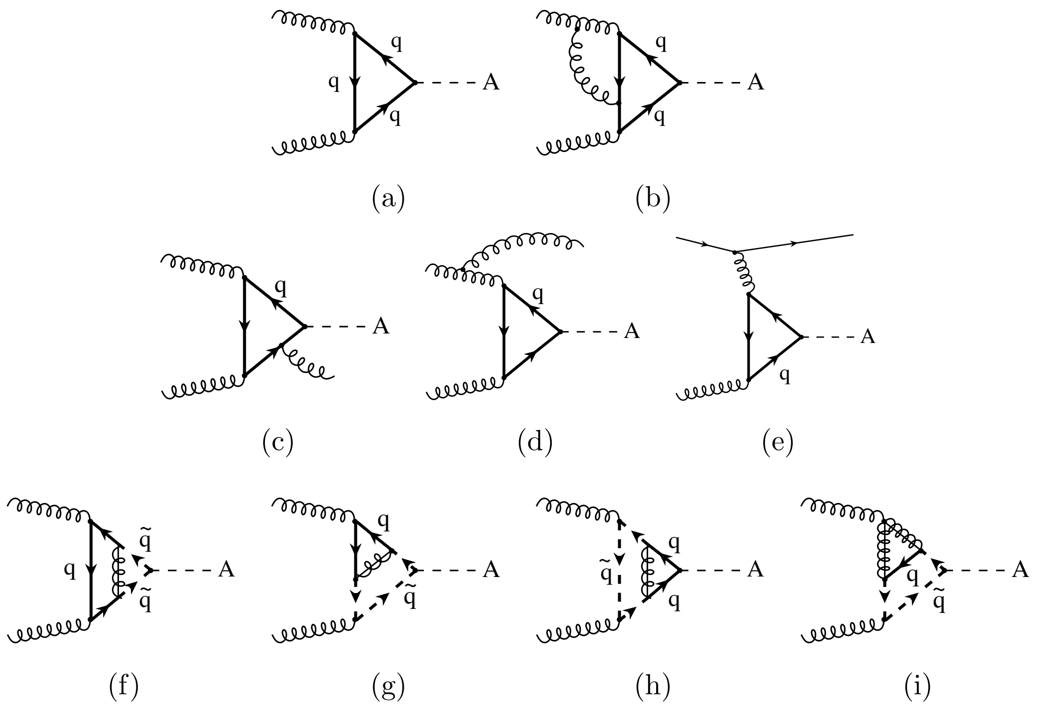

Figure 1: Diagrams contributing to the process $gg \to A + X$ in the MSSM at (a) LO and (b)–(i) NLO. According to the definition of the main text, (a)–(e) are referred to as "SM diagrams", (f)–(i) as "SUSY diagrams". The straight-curly line connecting quarks and squarks represents a gluino (denoted by $\tilde{g}$ in the text).

2.3 Standard Model limit and leading order result

In the limit where all SUSY masses tend to infinity (denoted in the following by $M_{\rm SUSY} \to \infty$), the Lagrangian of Eq. (2.1) reduces to

$$\mathcal{L}^{\rm SM} = \mathcal{L}_{\rm QCD} + \mathcal{L}_{qA} \,. \tag{2.6}$$

This will be called the "Standard Model" limit in what follows, despite the fact that the SM does not contain a CP-odd Higgs boson. Consequently, diagrams without any squark and gluino lines will be called "SM diagrams" (e.g. Fig. 1 (a)–(e)), while "SUSY diagrams" contain at least one propagator of a SUSY particle[3] (Fig. 1 (f)–(i)).

[3] In the following we will strictly distinguish between SM/SUSY *diagrams* and SM/SUSY *results*: As it turns out, the SM diagrams do *not* give the SM result in our scheme.

Note that due to the antisymmetric structure of the $\tilde{g}^A_{q,ij}$, Eq. (2.4), there are no SUSY diagrams at the one-loop level. The LO result for the partonic process $gg \to A$ is thus determined solely by diagrams of the type shown in Fig. 1 (a). It reads explicitely:

$$\begin{aligned}
\hat{\sigma}_{gg}(x) &= \sigma_0^A\, \delta(1-x) + \mathcal{O}(\alpha_s^3)\,, \\
\sigma_0^A &= \frac{\pi}{256 v^2}\left(\frac{\alpha_s}{\pi}\right)^2 \left| \sum_{q\in\{t,b\}} \mathcal{A}_q(\tau_q)\right|^2 , \\
\mathcal{A}_q(\tau_q) &= g_q^A\, \tau_q f(\tau_q)\,, \qquad \tau_q = \frac{4m_q^2}{M_A^2}\,,
\end{aligned} \tag{2.7}$$

where

$$f(\tau) = \begin{cases} \arcsin^2 \dfrac{1}{\sqrt{\tau}}\,, & \tau \geq 1\,, \\ -\dfrac{1}{4}\left[\ln \dfrac{1+\sqrt{1-\tau}}{1-\sqrt{1-\tau}} - i\pi\right]^2 , & \tau < 1\,. \end{cases} \tag{2.8}$$

Throughout this paper, α_s denotes the strong coupling constant, renormalized in the $\overline{\text{MS}}$ scheme for QCD with five massless quark flavors.

3. Higher orders

3.1 Standard Model result – Effective Lagrangian

The SM contributions, based on $\mathcal{L}_{\rm SM}$ of Eq. (2.6), are known through NLO in terms of 1-dimensional integral representations [8], implemented in the program `HIGLU` [18]. They include both top and bottom quark loops as shown in Fig. 1 (a)–(e) ($q \in \{b,t\}$).

It has been shown in Ref. [8, 9] that the NLO top quark contributions are well approximated by the formula

$$\sigma_t^{\rm NLO} = K_\infty\, \sigma_t^{\rm LO}\,, \quad \text{where} \qquad K_\infty = \frac{\sigma_\infty^{\rm NLO}}{\sigma_\infty^{\rm LO}}\,. \tag{3.1}$$

σ_∞ is the cross section evaluated in an effective theory, obtained by integrating out the top quark:

$$\mathcal{L}_{\rm QCD} + \mathcal{L}_{qA} \overset{m_t \gg M_A}{\longrightarrow} \mathcal{L}_{ggA}^{\rm SM} = -\frac{A}{v}\left[\tilde{C}_1^{\rm SM}\, \tilde{\mathcal{O}}_1 + \tilde{C}_2^{\rm SM}\, \tilde{\mathcal{O}}_2\right] + \mathcal{L}_{\rm QCD}^{(5)}\,. \tag{3.2}$$

The operators are defined as

$$\tilde{\mathcal{O}}_1 = \frac{1}{4}\varepsilon^{\mu\nu\alpha\beta} G^a_{\mu\nu} G^a_{\alpha\beta}\,, \qquad \tilde{\mathcal{O}}_2 = \sum_{q\neq t} \partial_\mu \left(\bar{q}\gamma^\mu\, \gamma_5 q\right)\,. \tag{3.3}$$

Here, $\{q\} := \{d,u,s,c,b\}$ denotes the set of light (in our case massless) quark fields and $G^a_{\mu\nu}$ the gluon field strength tensor. $\mathcal{L}_{\rm QCD}^{(5)}$ is the Standard QCD Lagrangian with five quark flavors.

The Wilson coefficients $\tilde{C}_1^{\rm SM}$ and $\tilde{C}_2^{\rm SM}$ have been calculated through NNLO in Ref. [19]. $\tilde{C}_2^{\rm SM}$ contributes only at NNLO and shall not be discussed any further in this paper. The result for $\tilde{C}_1^{\rm SM}$ is

$$\tilde{C}_1^{\rm SM} = -\cot\beta\frac{\alpha_s}{16\pi} + \mathcal{O}(\alpha_s^4)\,, \tag{3.4}$$

as it had been previously suggested in Refs. [9, 20] on the basis of the Adler-Bardeen theorem [21].

$\tilde{\mathcal{O}}_1$ generates vertices which couple two and three gluons to the pseudo-scalar Higgs (the $ggggA$-vertex vanishes due to the Jacobi identity of the structure functions of SU(3)). Sample diagrams that contribute to the NLO cross section in the effective theory of Eq. (3.2) are shown in Fig. 2. The full set has been calculated through NLO in Ref. [8], and through NNLO in Ref. [3, 4, 6].

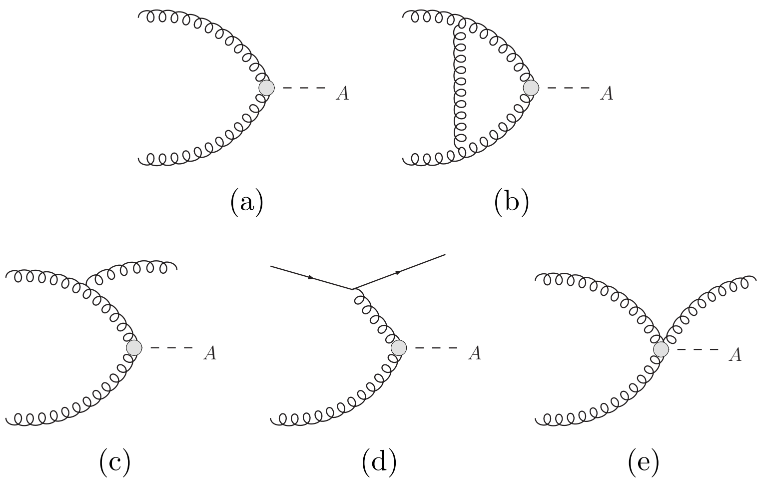

Figure 2: Diagrams contributing to the gluon fusion process in the effective theory at NLO.

3.2 SUSY contributions

We construct again an effective theory, this time by integrating out not only the top quark, but also all the SUSY particles. Since the remaining degrees of freedom are the same as in the Standard Model case of Sect. 3.1, the effective Lagrangian has exactly the same form as in Eq. (3.2), only with $\tilde{C}_1^{\rm SM}$ and $\tilde{C}_2^{\rm SM}$ replaced by $\tilde{C}_1$ and $\tilde{C}_2$.

As in the SM case, $\tilde{C}_2$ is zero through NLO. It remains to determine $\tilde{C}_1$ within the framework of Eq. (2.1) through NLO in α_s. The calculation of the SM case in Ref. [19] was done using dimensional regularization (DREG) as it is most convenient for loop calculations in QCD. However, it is known that DREG breaks SUSY and thus the formulae of Ref. [19] for the determination of $\tilde{C}_1$ cannot be applied to the full Lagrangian of Eq. (2.1) immediately.

A particularly subtle issue is the treatment of γ_5. Ref. [19] adopted the method of Ref. [13, 22, 23] which requires finite counter terms in order to restore gauge invariance [24]. These counter terms are not known for dimensionally regularized supersymmetry.

Therefore, we do not attempt to calculate the Feynman diagrams within DREG. Instead, we apply DRED [25] in order to regularize the divergent integrals. This is done by setting $D = 4$ after contracting all (Lorentz and spinor) indices [26, 27]. The loop integrals are subsequently evaluated in $D = 4 - 2\epsilon$ dimensions.

Both the pseudo-scalar vertex as well as the gluino-quark-squark vertices involve γ_5 matrices. We anticommute these γ_5 matrices and use $\gamma_5^2 = 1$ until only one of them remains in the Fermion trace. That one we replace by [13, 23, 19]

$$\gamma_5 = \frac{i}{4!}\varepsilon_{\mu\nu\rho\sigma}\gamma^{[\mu}\gamma^{\nu}\gamma^{\rho}\gamma^{\sigma]}\,. \tag{3.5}$$

It has been shown that the occurrence of the Levi-Civita symbol $\varepsilon_{\mu\nu\rho\sigma}$ can lead to inconsistencies when implemented in DRED [10]. We circumvent them by keeping the genuinely 4-dimensional Levi-Civita symbol $\varepsilon_{\mu\nu\rho\sigma}$ uncontracted until after the renormalization procedure, in close analogy to Refs. [23, 19]. As opposed to the calculation in DREG [19], however, working in DRED by definition does not involve terms of $\mathcal{O}(\epsilon = 2 - D/2)$ that require the above-mentioned finite counter terms in order to restore gauge invariance. Thus, the formulae of Ref. [19] for projecting onto the coefficient function $\tilde{C}_1$ can be translated to the DRED case by setting $D = 4$ and ignoring the finite renormalization of the pseudo-scalar current.[4]

Clearly, the SM diagrams alone will not yield the SM result of Eq. (3.4) in this way. However, we will explicitely demonstrate that this result is recovered (through $\mathcal{O}(\alpha_s^3)$) by making all the superpartner masses infinitely heavy *after* adding the results for *all* diagrams. This means that the SUSY diagrams lead to terms that do not vanish as $M_{\rm SUSY} \to \infty$. Rather, they combine with the result for the SM diagrams to give the correct SM result.

A rigorous proof of the validity of this approach through higher orders is very desirable, of course, because it greatly simplifies precision calculations in SUSY models as they might be required by future experimental data.

4. Results

The evaluation of the diagrams proceeds in complete analogy to Ref. [7]. At NLO, one needs to evaluate massive 2-loop diagrams with vanishing external momenta. This is possible in a fully analytic way with the help of the algorithm of Ref. [28][5]. As a cross check, we also calculated the diagrams in the limit $m_t \ll m_{\tilde{t}_1} \ll m_{\tilde{t}_2} \ll m_{\tilde{g}}$ by using automated asymptotic expansions [30] and found agreement with the corresponding expansion of the analytical result.

Subsequently, the bare coupling constant within the SUSY-QCD theory is transformed to its renormalized 5-flavor QCD expression in the $\overline{\rm MS}$ scheme as described in Ref. [7].

[4]In the notation of Ref. [19] this means $Z_5^p \equiv 1$.

[5]We are indepted to M. Steinhauser for providing us with his implementation of this algorithm in the framework of `MATAD` [29].

In DRED, and using the prescription for the treatment of γ_5 described above, we find the following contribution of all SM diagrams to the coefficient function:

$$\tilde{C}_1\big|_{\text{SM-dias}} = -\frac{\alpha_s}{16\pi}\cot\beta\left\{1 - \frac{2}{3}\frac{\alpha_s}{\pi}\right\} + \mathcal{O}(\alpha_s^3)\,. \tag{4.1}$$

As expected, it differs from the well-known result of Eq. (3.4). The SUSY diagrams, on the other hand, add up to

$$\tilde{C}_1\big|_{\text{SUSY-dias}} = -\frac{\alpha_s}{16\pi}\cot\beta\left\{\frac{2}{3}\frac{\alpha_s}{\pi}\right\} + \mathcal{O}(\frac{m_t^2}{M^2}) + \mathcal{O}(\alpha_s^3)\,, \qquad M \in \{m_{\tilde{t}}, m_{\tilde{g}}\}\,, \tag{4.2}$$

such that indeed the SM limit is recovered as the SUSY masses are decoupled:

$$\tilde{C}_1^{\text{SM}} = \lim_{M_{\text{SUSY}}\to\infty}\left(\tilde{C}_1\big|_{\text{SM-dias}} + \tilde{C}_1\big|_{\text{SUSY-dias}}\right)\,. \tag{4.3}$$

We are not aware of a calculation where this interplay between DRED and γ_5 in a SUSY theory has been observed before.

The general NLO result for $\tilde{C}_1$ can then be cast into the following form:

$$\tilde{C}_1^{\text{SM}} = -\frac{\alpha_s}{16\pi}\cot\beta\left\{1 + \frac{\alpha_s}{\pi}\frac{\mu_{\text{SUSY}}}{m_{\tilde{g}}}\left(\cot\beta + \tan\beta\right)\, f(m_t, m_{\tilde{t}_1}, m_{\tilde{t}_2}, m_{\tilde{g}})\right\} + \mathcal{O}(\alpha_s^3)\,. \tag{4.4}$$

A few observations may be worth pointing out:

- Eq. (4.4) immediately shows that the NLO corrections to the coefficient function will get more important w.r.t. the LO term for large values of $\tan\beta$ and μ_{SUSY}. On the other hand, large values of $\tan\beta$ increase the importance of bottom contributions even more, so that they usually obscure the squark effects. This will be shown explicitely for the SPS 1a scenario in Sect. 5.

- The squark mixing angle θ_t, though present in individual diagrams, drops out in the final result.

- Due to the absence of mass terms at LO, the explicit form of f is independent of the mass renormalization scheme.

The general result for $f(m_t, m_{\tilde{t}_1}, m_{\tilde{t}_2}, m_{\tilde{g}})$ is too voluminous to be displayed here. Instead, we implemented $\tilde{C}_1$ in the program `evalcsusy.f` [7][6] and analyze its behavior numerically as shown in Sect. 5.

For practical purposes, it might be useful to provide the analytical expression of the function f for some limiting cases. For example, if all masses are set equal,

$$m_t = m_{\tilde{t}_1} = m_{\tilde{t}_2} = m_{\tilde{g}} =: M\,, \tag{4.5}$$

[6] The program is available from `http://www-ttp.physik.uni-karlsruhe.de/Progdata/ttp04/ttp04-19`.

we obtain

$$f(M,M,M,M) = \frac{5}{18} - \frac{9}{2}\,S_2 = -0.894176\ldots\,, \tag{4.6}$$

where $S_2 = 4\,\mathrm{Cl}_2\,(\pi/3)\,/(9\sqrt{3})$ has been inserted.

On the other hand, assuming

$$m_t = m_{\tilde t_1} = m_{\tilde t_2} =: M \ll m_{\tilde g}\,, \tag{4.7}$$

we find

$$\begin{aligned} f(M,M,M,m_{\tilde g}) &= \frac{2}{3} + \frac{2}{3}\,l_g + x_g\left(\frac{7}{6} - \frac{1}{3}\,\zeta_2 + \frac{13}{6}\,l_g - \frac{1}{6}\,l_g^2\right) + \mathcal{O}(x_g^2)\,,\\ x_g &= \frac{M^2}{m_{\tilde g}^2}\,, \qquad l_g = \ln x_g\,, \qquad \zeta_2 = \frac{\pi^2}{6}\,. \end{aligned} \tag{4.8}$$

Insertion into Eq. (4.4) shows that, in contrast to scalar Higgs production [31, 32, 7], the result for $\tilde C_1$ is well-behaved as $m_{\tilde g} \to \infty$ at finite M. This is because there are no squark contributions at LO which could affect the renormalization of the NLO terms.

For completeness, let us also give the result for the somewhat unphysical case

$$m_t \gg m_{\tilde t_1} = m_{\tilde t_2} = m_{\tilde g} =: M\,, \tag{4.9}$$

where f assumes the form

$$\begin{aligned} f(m_t,M,M,M) &= \frac{3}{2} + \frac{3}{2}\,l_t + x_t\left(\frac{11}{3} + 3\,\zeta_2 + \frac{29}{3}\,l_t + \frac{3}{2}\,l_t^2\right) + \mathcal{O}(x_t^2)\,,\\ x_t &= \frac{M^2}{m_t^2}\,, \qquad l_t = \ln x_t\,. \end{aligned} \tag{4.10}$$

5. Discussion

5.1 Coefficient function $\tilde C_1$

We will now discuss the numerical effect of the newly evaluated terms. First, we investigate the dependence of $\tilde C_1$ on the squark and gluino masses. To this aim, it is convenient to consider the leading and the NLO term separately:

$$\tilde C_1 = -\frac{\alpha_s}{16\pi}\left(\tilde c_1^{(0)} + \frac{\alpha_s}{\pi}\,\tilde c_1^{(1)}\right) + \mathcal{O}(\alpha_s^3)\,. \tag{5.1}$$

According to Eq. (4.4),

$$\tilde c_1^{(0)} = \cot\beta\,. \tag{5.2}$$

Fig. 3 shows $\tilde c_1^{(1)}$ as a function of $m_{\tilde g}$ for various values of $m_{\tilde t_1}$ and $m_{\tilde t_2}$. In Fig. 4, on the other hand, we consider it as a function of $m_{\tilde t_2}$ and fix $m_{\tilde g}$ and $m_{\tilde t_1}$ at a few representative values. Note that $\tilde{c}_1^{(1)}$ is symmetric in $m_{\tilde{t}_1}$ and $m_{\tilde{t}_2}$ since it does not depend on θ_t as mentioned above. In Fig. 5, $m_{\tilde{t}_1} = m_{\tilde{t}_2} = m_{\tilde{t}}$ is varied for certain choices of $m_{\tilde{g}}$. And finally, in Fig. 6 we adopt the benchmark scenario SPS1a of Ref. [33] and consider $\tilde{c}_1^{(0)}$ and $\tilde{c}_1^{(1)}$ as functions of $m_{1/2}$. In this case, the corresponding low energy parameters can be evaluated with the help of a SUSY spectrum calculator [34, 35, 36].[7]

The general structure is quite similar in all figures: $\tilde{c}_1^{(1)}$ is of the order of 0.5 for moderate values of the SUSY masses. As they increase, $\tilde{c}_1^{(1)}$ tends to zero in agreement with the general discussion above. In order to demonstrate this behavior more clearly, Fig. 7 adopts the same parameters as Fig. 3, but extends up to very large values of the gluino mass.

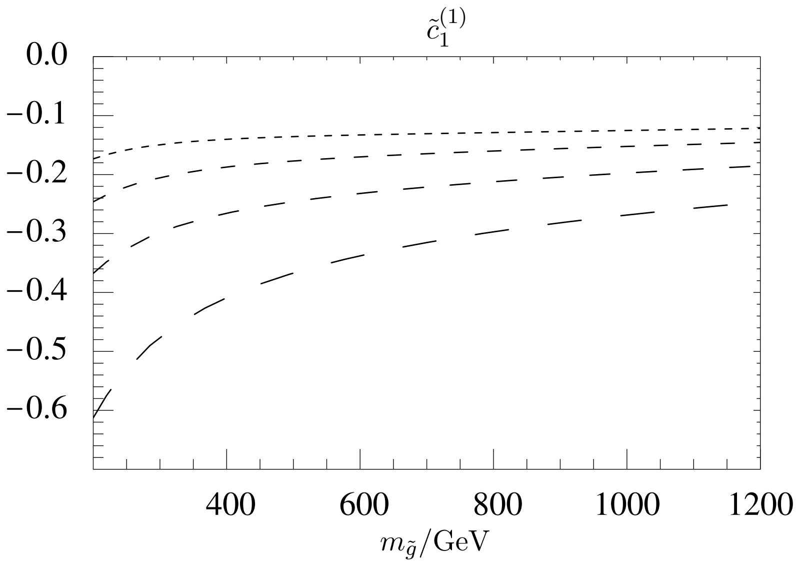

Figure 3: $\tilde{c}_1^{(1)}$ as a function of the gluino mass for $m_t = 178\,\text{GeV}$, $\mu_{\text{SUSY}} = 150\,\text{GeV}$, $\tan\beta = 10$, and $(m_{\tilde{t}_1}, m_{\tilde{t}_2}) = (200, 200)/(200, 400)/(200, 600)/(400, 600)\,\text{GeV}$ [long/.../short dashes].

5.2 Cross section

The inclusive NLO hadronic cross section for pseudo-scalar Higgs production receives contributions from the subprocesses $gg \to A(+g)$, $qg \to Aq$, and $q\bar{q} \to Ag$. At this order, squarks only affect the process $gg \to A$, because of the antisymmetric structure of the $\tilde{q}_i\tilde{q}_j A$ coupling, cf. Eqs. (2.2), (2.4). Recalling the notation of Eq. (2.5), we write

$$\hat{\sigma}_{gg}(x) = \hat{\sigma}_{tb}(x) + \Delta\hat{\sigma}_{\tilde{t}t}(x) + \Delta\hat{\sigma}_{\tilde{t}b}(x) + \mathcal{O}(\alpha_s^4)\,, \tag{5.3}$$

where $\hat{\sigma}_{tb}$ denotes the contributions arising from the top and bottom mediated gluon-Higgs couplings. It can be evaluated through NLO for arbitrary top, bottom, and Higgs masses with the help of the `FORTRAN` program `HIGLU`. The same is true for the qg sub-process (see Fig. 1 (e)).

[7] We use `SoftSusy` [34] in this paper.

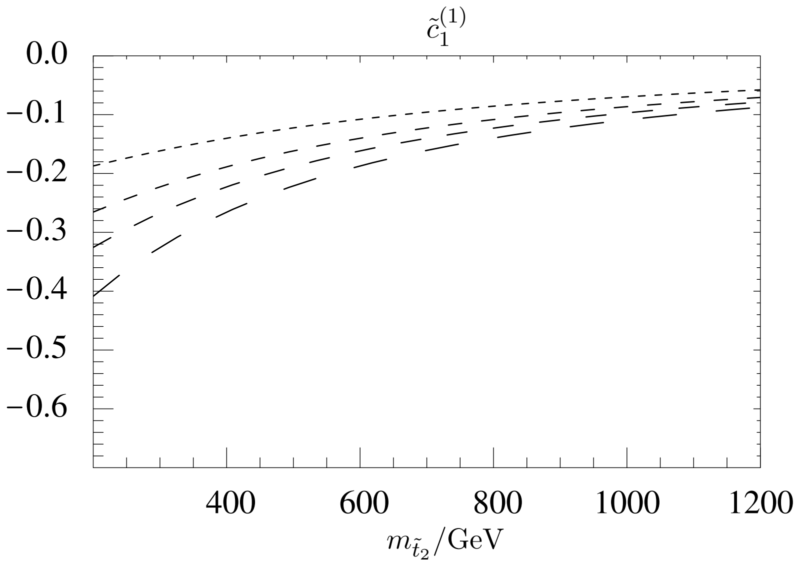

Figure 4: $\tilde{c}_1^{(1)}$ as a function of $m_{\tilde{t}_2}$ for $m_t = 178\,\text{GeV}$, $\mu_{\text{SUSY}} = 150\,\text{GeV}$, $\tan\beta = 10$, $m_{\tilde{g}} = 400\,\text{GeV}$, and $m_{\tilde{t}_1} = 200/300/400/600\,\text{GeV}$ [long/.../short dashes].

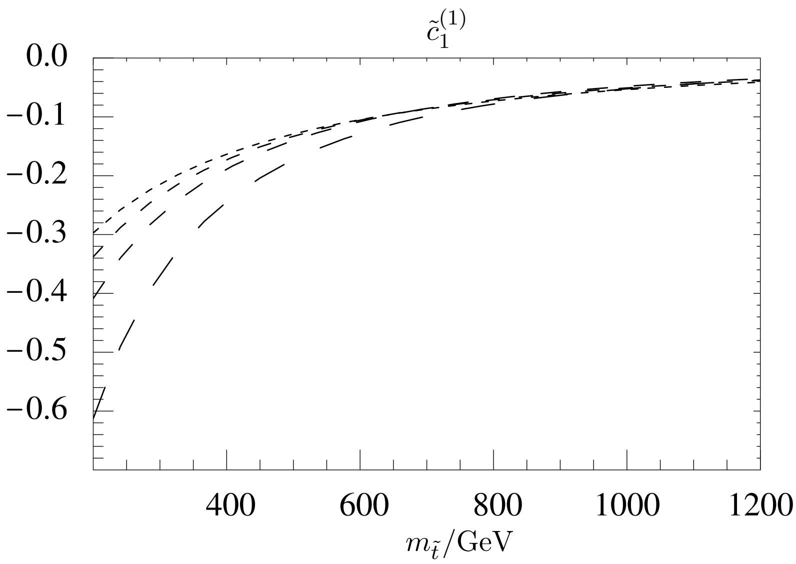

Figure 5: $\tilde{c}_1^{(1)}$ as a function of $m_{\tilde{t}} \equiv m_{\tilde{t}_1} = m_{\tilde{t}_2}$ for $m_t = 178\,\text{GeV}$, $\mu_{\text{SUSY}} = 150\,\text{GeV}$, $\tan\beta = 10$, $m_{\tilde{g}} = 200/400/600/800\,\text{GeV}$ [long/.../short dashes].

$\Delta\hat{\sigma}_{\tilde{t}t}$ and $\Delta\hat{\sigma}_{\tilde{t}b}$ are the effects arising from the interference of stop-induced with top- and bottom-induced amplitudes:

$$\Delta\hat{\sigma}_{\tilde{t}q} \sim \text{Re}\left(\mathcal{M}_{\tilde{t}}^{(1)*}\mathcal{M}_q^{(0)}\right)\,, \qquad q \in \{b,t\}\,. \tag{5.4}$$

$\mathcal{M}_q^{(0)}$ is expressed in terms of $\mathcal{A}_q$ from Eq. (2.8), while for $\mathcal{M}_{\tilde{t}}^{(1)}$, we use the expression evaluated in the effective theory to obtain

$$\Delta\hat{\sigma}_{\tilde{t}q}(x) = \frac{\pi}{128v^2}\left(\frac{\alpha_s}{\pi}\right)^3 \text{Re}\left(\tilde{c}_1^{(1)}\,\mathcal{A}_q(\tau_q)\right)\,\delta(1-x)\,. \tag{5.5}$$

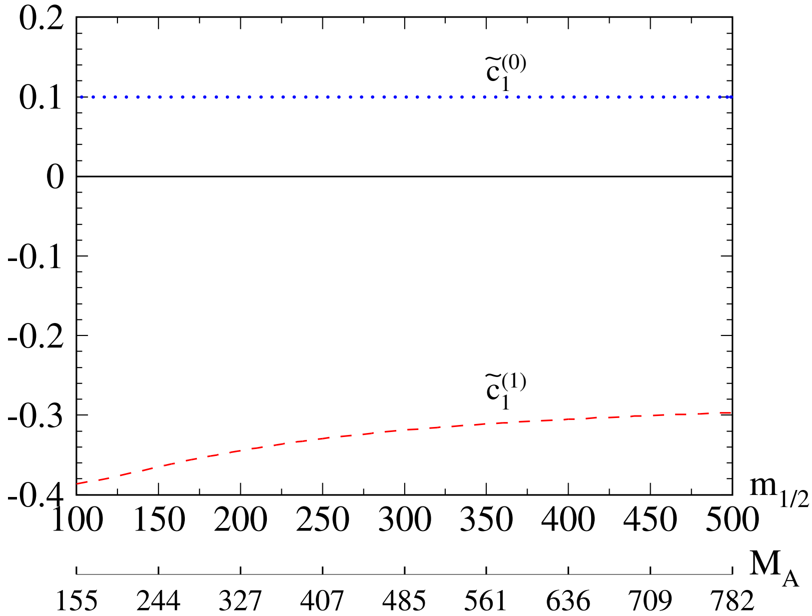

Figure 6: LO and NLO contribution to the coefficient function $\tilde{C}_1$ as defined in Eq. (5.1) for the SPS1a scenario.

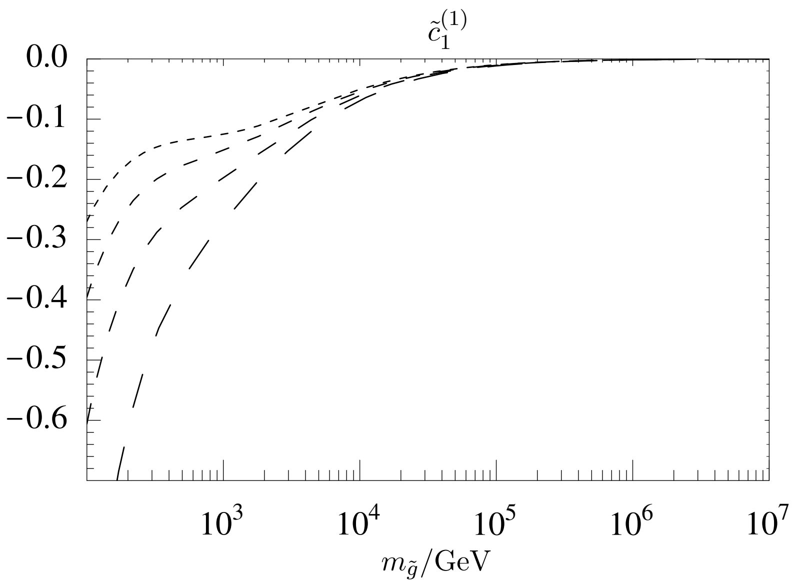

Figure 7: Same as Fig. 3, but extended abscissa in order to demonstrate the asymptotic behavior of $\tilde{c}_1^{(1)}$.

Note that $\mathcal{M}_{\tilde{t}}^{(1)}$ has a branch cut at $M_A = 2m_t$. Thus, we expect our result to be valid for $M_A < 2m_t$. Recall, however, that in the SM case, the heavy top limit still provides an excellent approximation for Higgs masses much larger than $2m_t$ [8, 9, 37].

To study the numerical effects, we consider the SPS1a scenario. In a first step, the bottom quark Yukawa coupling will be switched off for illustrational purposes. Fig. 8 then shows the NLO K-factor with and without the top-stop interference term $\Delta\hat{\sigma}_{\tilde{t}t}$. The effect of the SUSY contributions is a decrease in the NLO cross section by up to 10% for $M_A < 2m_t$, which is indeed significantly larger than for the case of scalar Higgs production [7] due to the absence of higher order SM corrections to $\tilde{C}_1$.

Taking into account bottom quark effects overshadows most of this shift as shown in Fig. 9. On the one hand, this is due to the large size of the pure bottom quark contributions. On the other hand, the top-stop and bottom-stop interference terms are almost equal in magnitude, but opposite in sign, as illustrated in Fig. 10. This means that, like in the case of scalar Higgs production, the higher order corrections are accounted for fairly precisely by rescaling the LO result with the SM K-factor.

Finally, Fig. 11 shows the inclusive cross section through NLO for the SPS 1a scenario, including effects of top and bottom quarks as well as top squarks.[8]

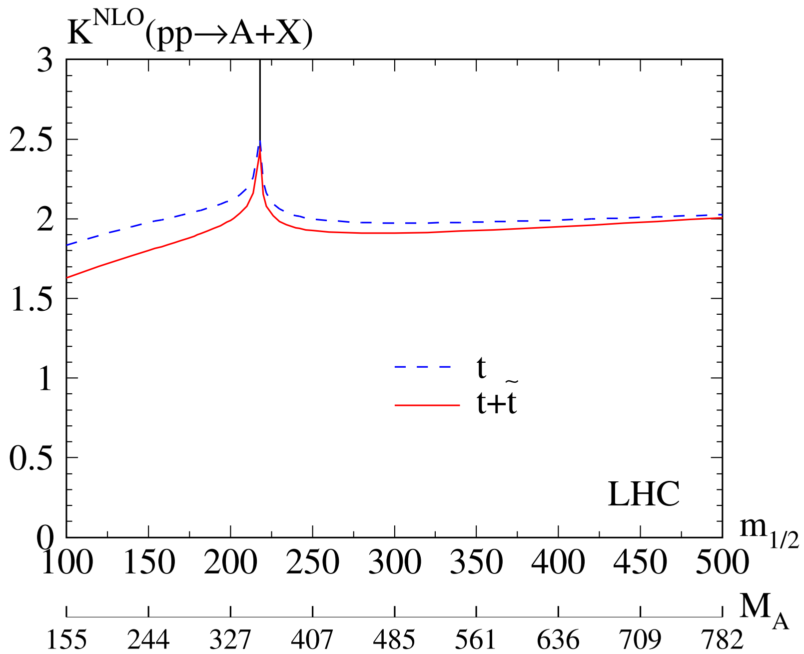

Figure 8: NLO K-factor, taking into account only top quark loops (dashed) and adding the top-stop interference contributions (solid).

6. Conclusions

The corrections to the effective Higgs-gluon coupling for pseudo-scalar Higgs bosons have been evaluated in the MSSM through first order in the strong coupling constant α_s. The numerical effects were studied within a specific SUSY scenario (SPS 1a); further studies

[8] The singularity at $M_A = 2m_t$ in Figs. 8, 9, and 11 is due to the threshold behavior of the NLO quark contribution [8, 9].

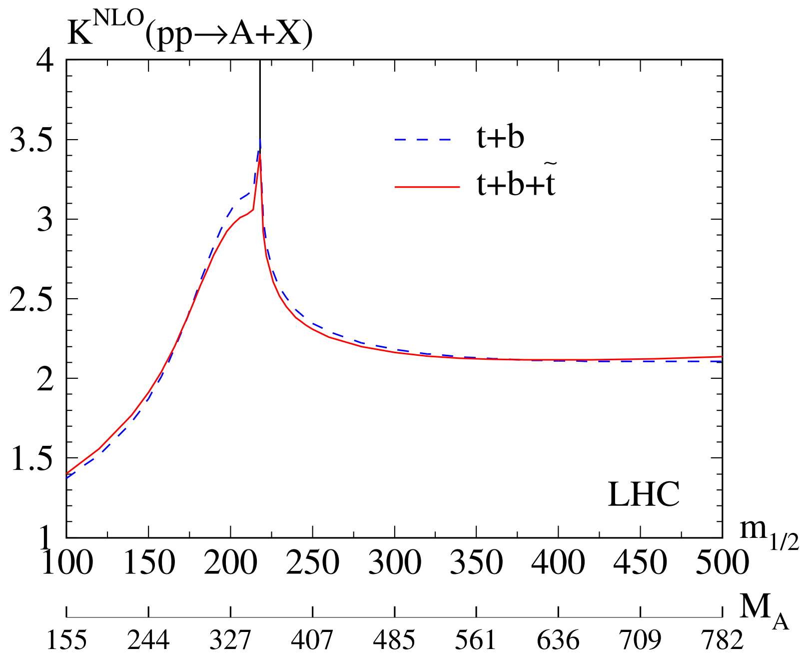

Figure 9: K-factor, taking into account top- and bottom-quark loops (dashed), and adding the top-stop and bottom-stop interference contributions (solid).

can be performed easily using the publicly available numerical routine `evalcsusy.f` (see footnote on page 8).

The calculation also addresses a technical issue, since it involves the γ_5 matrix in a non-trivial way. In analogy to Ref. [19], we avoided the contraction of the Levi-Civita symbol with D dimensional quantities. We argued that the calculation in DRED does not require finite counter terms as opposed to the DREG approach, provided the underlying theory is supersymmetric. Indeed, we observe a non-trivial cancellation of regularization scheme dependent terms among the SM and SUSY diagrams, such that the limit of an infinitely heavy SUSY spectrum is consistent with the well-known SM result.

It would be interesting to investigate these observations in more detail, in particular to prove the validity of our implementation of γ_5 within DRED in a rigorous way. Further corroboration could be obtained from its application at second order α_s. This corresponds to the evaluation of $\tilde{C}_1$ at three loops for which the technical tools are in principle available [38].

From the phenomenological point of view, one could calculate the photonic decay rate of the CP-odd Higgs boson in a very similar fashion. There, however, one does not need to rely strictly on the effective Lagrangian, but could evaluate the first few terms of a Taylor expansion in M_A^2/M^2 along the lines of Ref. [39], where $M \in \{m_t, m_{\tilde{t}}, m_{\tilde{g}}\}$.

Acknowledgments. Our thanks go to K. Chetyrkin, A. Djouadi, and J. Kühn for encouragement and inspiring conversations. We are grateful to M. Steinhauser for enlight-

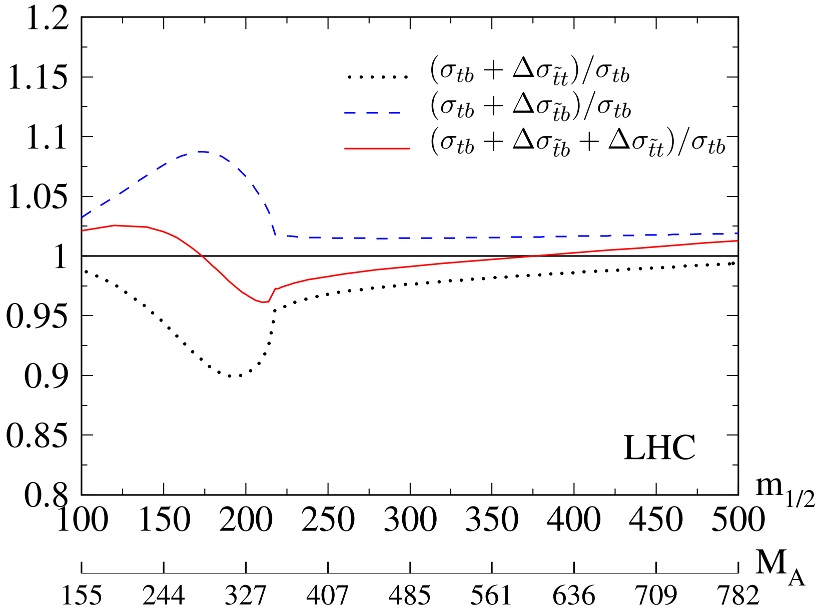

Figure 10: Relative effect of the top-stop (dotted) and bottom-stop (dashed) interference terms, as well as their sum (solid).

ening discussions concerning the treatment of γ_5, and D. Stöckinger for his constructive comments on the manuscript.

References

[1] A. Djouadi, `arXiv:hep-ph/0503172`; `arXiv:hep-ph/0503173`.

[2] R.V. Harlander and W.B. Kilgore, *Phys. Rev. Lett.* **88**, 201801 (2002).

[3] R.V. Harlander and W.B. Kilgore, *JHEP* **0210**, 017 (2002).

[4] C. Anastasiou and K. Melnikov, *Phys. Rev.* **D 67**, 037501 (2003).

[5] C. Anastasiou and K. Melnikov, *Nucl. Phys.* **B 646**, 220 (2002).

[6] V. Ravindran, J. Smith, W.L. van Neerven, *Nucl. Phys.* **B 665**, 325 (2003).

[7] R.V. Harlander and M. Steinhauser, *JHEP* **0409**, 066 (2004).

[8] M. Spira, A. Djouadi, D. Graudenz, P.M. Zerwas, *Nucl. Phys.* **B 453**, 17 (1995).

[9] M. Spira, *Fortschr. Phys.* **46**, 203 (1998).

[10] W. Siegel, *Phys. Lett.* **B 94**, 37 (1980).

[11] J. Smith and W.L. van Neerven, *Eur. Phys. J.* **C 40**, 199 (2005).

[12] D. Stöckinger, *JHEP* **0503**, 076 (2005).

[13] G. 't Hooft and M.J. Veltman, *Nucl. Phys.* **B 44**, 189 (1972).

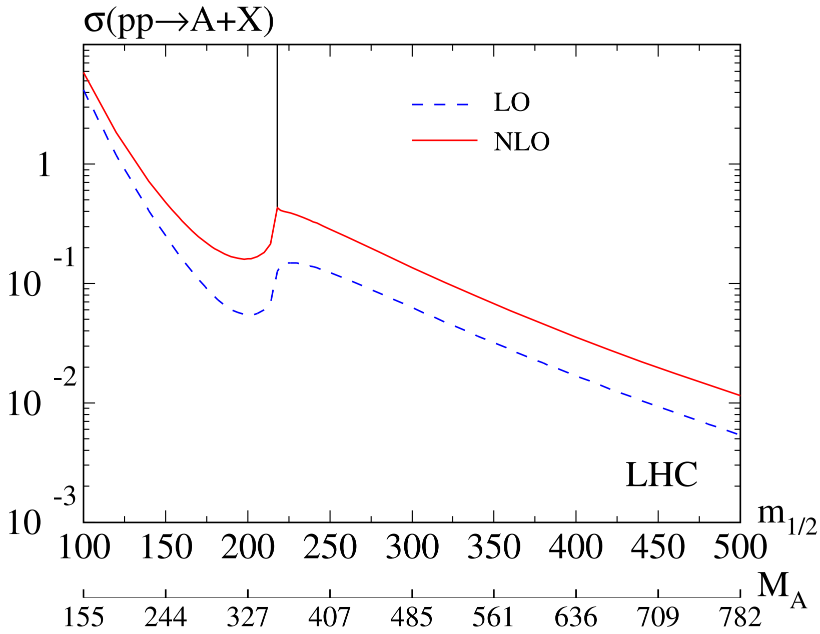

Figure 11: Total cross section including top, bottom, and stop effects through LO (dashed) and NLO (solid).

[14] P. Breitenlohner and D. Maison, *Comp. Phys. Commun.* **52**, 11 (1977).

[15] S. Kraml, PhD thesis, Vienna University (1999), `arXiv:hep-ph/9903257`.
H. Eberl, PhD thesis, Vienna University (1998).

[16] A.D. Martin, R.G. Roberts, W.J. Stirling, R.S. Thorne, *Eur. Phys. J.* **C 23**, 73 (2002).

[17] A.D. Martin, R.G. Roberts, W.J. Stirling, R. S. Thorne, *Eur. Phys. J.* **C 35**, 325 (2004).

[18] M. Spira, `arXiv:hep-ph/9510347`.

[19] K.G. Chetyrkin, B.A. Kniehl, M. Steinhauser, W.A. Bardeen, *Nucl. Phys.* **B 535**, 3 (1998).

[20] M. Krämer, E. Laenen, M. Spira, *Nucl. Phys.* **B 511**, 523 (1998).

[21] S.L. Adler and W.A. Bardeen, *Phys. Rev.* **182**, 1517 (1969).

[22] D.A. Akyeampong and R. Delbourgo, *Nuovo Cim.* **17A**, 578 (1973).

[23] S.A. Larin, *Phys. Lett.* **B 303**, 113 (1993).

[24] T.L. Trueman, *Phys. Lett.* **B 88**, 331 (1979).

[25] W. Siegel, *Phys. Lett.* **B 84**, 193 (1979).

[26] I. Jack, D.R.T. Jones, K.L. Roberts, *Z. Phys.* **C 63**, 151 (1994).

[27] I. Jack and D.R.T. Jones, `arXiv:hep-ph/9707278`.

[28] A.I. Davydychev and J.B. Tausk, *Nucl. Phys.* **B 397**, 123 (1993).

[29] M. Steinhauser, *Comp. Phys. Commun.* **134**, 335 (2001).

[30] T. Seidensticker, `arXiv:hep-ph/9905298`.
R. Harlander, T. Seidensticker, M. Steinhauser, *Phys. Lett.* **B 426**, 125 (1998).

[31] R.V. Harlander and M. Steinhauser, *Phys. Lett.* **B 574**, 258-268 (2003).

[32] R.V. Harlander and M. Steinhauser, *Phys. Rev.* **D 68**, 111701 (2003).

[33] B.C. Allanach *et al.*, in *Proc. of the APS/DPF/DPB Summer Study on the Future of Particle Physics (Snowmass 2001)* ed. N. Graf, *Eur. Phys. J.* **C 25**, 113 (2002), [eConf **C010630** (2001) P125].

[34] B.C. Allanach, *Comp. Phys. Commun.* **143**, 305 (2002).

[35] W. Porod, *Comp. Phys. Commun.* **153**, 275 (2003).

[36] A. Djouadi, J. L. Kneur, G. Moultaka, `arXiv:hep-ph/0211331`.

[37] R. Harlander, `arXiv:hep-ph/0311005`.

[38] R. Harlander and M. Steinhauser, *Prog. Part. Nucl. Phys.* **43**, 167 (1999).

[39] M. Steinhauser, `arXiv:hep-ph/9612395`.